THE JOURNAL OF PHYSICAL CHEMISTRY B

Article

pubs.acs.org/JPCB

Photoionization and Electron Radical Recombination Dynamics in Photoactive Yellow Protein Investigated by Ultrafast Spectroscopy in the Visible and Near-Infrared Spectral Region

Jingyi Zhu,[†] Laura Paparelli,[†] Marijke Hospes,[‡] Jos Arents,[‡] John T. M. Kennis,[†] Ivo H. M. van Stokkum,[†] Klaas J. Hellingwerf,[‡] and Marie Louise Groot*[,†]

[†]Department of Physics and Astronomy, Faculty of Sciences, VU University, De Boelelaan 1081, 1081 HV Amsterdam, The Netherlands

[‡]Laboratory for Microbiology, Swammerdam Institute for Life Sciences, University of Amsterdam, Science Park 904, 1098 XH Amsterdam, The Netherlands

Supporting Information

ABSTRACT: Photoinduced ionization of the chromophore inside photoactive yellow protein (PYP) was investigated by ultrafast spectroscopy in the visible and near-infrared spectral regions. An absorption band that extended from around 550 to 850 nm was observed and ascribed to solvated electrons, ejected from the *p*-hydroxycinnamic acid anion chromophore upon the absorption of two 400 nm photons. Global kinetic analysis showed that the solvated electron absorption decayed in two stages: a shorter phase of around 10 ps and a longer phase of more than 3 ns. From a simulation based on a diffusion model we conclude that the diffusion rate of the electron is about 0.8 Å^2/ps in wild type PYP, and that the electron is ejected to a short distance of only several angstroms away from the chromophore. The chromophore−protein pocket appears to provide a water-similar local environment for the electron. Because mutations at different places around the chromophore have different effect on the electron recombination dynamics, we suggest that solvated electrons could provide a new method to investigate the local dielectric environment inside PYP and thus help to understand the role of the protein in the photoisomerization process.

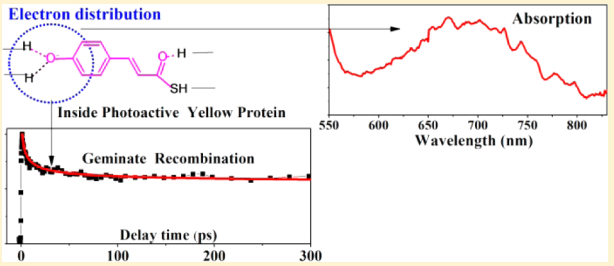

INTRODUCTION

Photoactive yellow protein (PYP) is a blue-light photoreceptor responsible for the negative phototaxis of the bacterium *Halorhodospira halophila*.[1−3] It is a convenient model system for studying chromophore photochemistry due to its small size, water solubility, and good optical stability.[4] The chromophore inside PYP, the *p*-hydroxycinnamic acid (pCa) anion covalently linked to the side chain of cysteine 69 via a thioester bond, has an absorption centered at 445 nm, as shown in Figure 1. Upon excitation, the pCa undergoes trans to cis isomerization around the C_7═C_8 bond,[5] initiating a photocycle that spans a time scale from subpicoseconds to seconds involving a series of photoproduct intermediate states.[6−8]

The quantum yield of isomerization in wild-type PYP is ∼35%.[9−11] At high excitation intensity, an extra, two-photon reaction channel opens up, resulting in electron ejection from the chromophore.[12,13] The negatively charged chromophore in PYP (Figure 1) has a low ionization potential (IP)[14,15] that is accessible via the energy provided by two 400 nm photons. This provides an opportunity to study photoionization and electron-radical recombination dynamics in a protein pocket environment. Although photoionization or photodetachment of an electron from an anion in solvent has been extensively studied in the past years,[16−23] studies of ionization or electron-

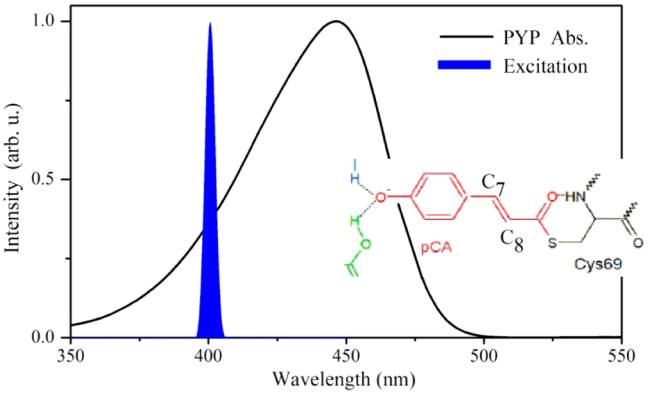

Figure 1. Steady-state absorption spectrum of wild-type PYP and spectrum of the laser pulse used for excitation in the pump−probe experiments. The inset shows the structure of the pCa chromophore inside PYP. Note that a negative charge resides on the phenolate oxygen of the chromophore.

Special Issue: Rienk van Grondelle Festschrift

Received: December 4, 2012
Revised: February 13, 2013

   dx.doi.org/10.1021/jp311906f | *J. Phys. Chem. B* XXXX, XXX, XXX−XXX

detachment from a chromophore in a protein pocket environment are quite rare. Characterization of the spectroscopy and dynamics of the solvated electron may shed light on the dielectrics in the protein and thereby enhance our understanding of the role of the protein in isomerization.[24] Furthermore, although PYP has good optical stability, at high, pulsed-light intensities this may be deteriorated due to photoionization. Therefore, a good characterization of the dynamics of recombination is of considerable interest, in view of possible device applications of PYP.[25] Because of the overlapping absorption bands of the electron and of the isomerized chromophore (I_0 and I_1), the shape of the electron band and its dynamics have not been characterized in the visible wavelength region in previous studies.

In the present study, we focused on the ionization in PYP and the electron-radical recombination dynamics by monitoring the full solvated electron band in the visible-near-infrared spectral region. Kinetic model analysis was applied to separate the spectra and dynamics of the solvated electron from that of the isomerization dynamics of the chromophore. Simulation of the geminate recombination dynamics based on diffusion theory was used to characterize the dynamics of the liberated electron and the initial distribution of the ejected electrons inside the protein pocket. The effects of selected amino acid residues on the electron recombination dynamics were studied using different mutants.

MATERIAL AND METHODS

Sample Preparation. Wild-type and mutant PYPs were expressed and isolated as described in the literature.[26] The purified holoproteins were used without the removal of the genetically introduced N-terminal hexa-histidine-containing tag in 20 mM Tris−HCl, pH 8.1. Site-directed mutagenesis was performed using the QuikChange kit (Stratagene, La Jolla, CA) and confirmed by DNA sequencing, as previously described.[27]

Transient Spectroscopy Measurements. The absorption difference spectra and ultrafast dynamics were recorded in a femtosecond transient absorption setup[28] based on a regenerative Ti:sapphire amplifier operating at 1 kHz (Legend Ultrashort Pulse Stretcher and Compressor, Coherent), which generated 50 fs pulses of several mJ/pulse, centered at a wavelength of 800 nm. One part of the fundamental pulse was chopped every other pulse and frequency-doubled to 400 nm with BBO crystal and used for excitation. The white-light probe in the UV−visible region was generated by focusing part of the fundamental 800 nm output on a laterally rotating 2 mm CaF_2 plate. The probe light in the visible-NIR region was generated by tuning an optical parametric amplifier opera solo (TOPAS, Coherent) pumped at 800 nm, to 1000 nm, and focusing the output in a 2 mm sapphire plate with a f = 5 cm lens. White light generated by this wavelength had a broad and smooth spectrum covering from 500 to 900 nm. After interrogation of the sample, the white light was dispersed in a spectrograph and detected on a 256-element diode array (model no. S4801-256Q; Hamamatsu, Hamamatsu City, Japan) read out at 1 kHz. The polarization of the excitation pulse was at the magic angle with respect to the probe pulse. Excitation intensity was measured with a power meter (3sigma, Coherent) and attenuated with a circular neutral density filter. For measuring in the UV−visible region, the concentration of the PYP sample was adjusted to an optical density (OD) of ∼0.7 at 445 nm in a CaF_2 cell of 30 μm path length. For measurements on the electron absorption band in the NIR, the same concentration of sample was used but incubated in a CaF_2 cell of 150 μm path length. The sample cells were contained in a Lissajous sample scanner. The scanner was moved at such speed that a new part of the sample was illuminated at every shot. The integrity of the sample was determined by measuring its absorption spectrum before and after experiments.

Data Analysis. Broad-band femtosecond transient absorption data were analyzed by globally fitting all of the wavelength dynamics with shared rate constants from a kinetic model.[29] Details of this method and analysis of the data with lower excitation energy are described in the Supporting Information. Simulations based on a diffusion model were performed with Labview programmed code.

RESULTS AND DISCUSSION

Figure 2A presents transient spectra at selected delay times for wild-type PYP. In the wavelength region below 550 nm,

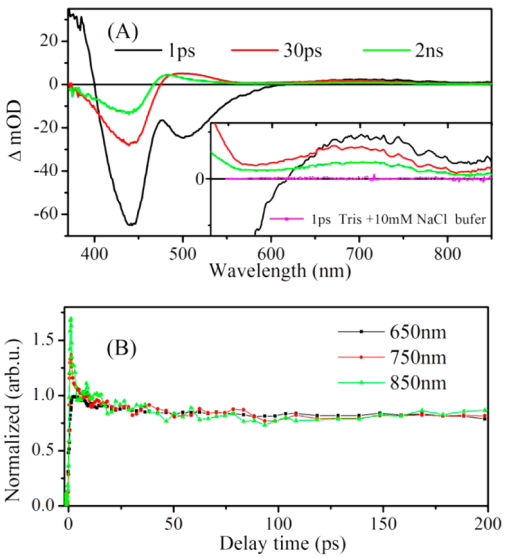

Figure 2. (A) Dispersion-corrected transient spectra of wild-type PYP at different delay times after excitation. Note that the broad spectra were collected in two spectral windows and were normalized to each other in the overlapping region around 580 nm. The excitation intensity was ∼1.1 × 10^{15} photons/cm^2 at 400 nm. (B) Normalized decay curves at selected wavelengths.

consistent with previous observations,[5,12,30,31] the spectra consisted of excited-state absorption below 400 nm (1 ps), ground-state bleach around 450 nm, stimulated emission around 500 nm (1 ps), and isomerized product absorption around 500 nm (30 ps and 2 ns). Above 550 nm, a broad absorption band (1 ps) was observed, which overlapped with the stimulated emission tail of the excited state. At long delay times, as the stimulated emission disappeared the shape of this absorption band became clearer: It extended from around 550 to 850 nm with a center at 700 nm. The decay dynamics of this band at different wavelengths are shown in Figure 2B; they display a uniform decay in the long time range. The shape of this absorption band and its dynamics is similar to that of solvated electrons observed in other systems,[20,32−34] with only little broadening or shifting. Moreover, this spectrum is strikingly similar to the terminal spectrum measured after photoionization of the isolated PYP chromophore in solution.[21−23] Nevertheless, to rule out the possibility of multiphotoionization of water or buffer molecules, we repeated

dx.doi.org/10.1021/jp311906f | J. Phys. Chem. B XXXX, XXX, XXX−XXX

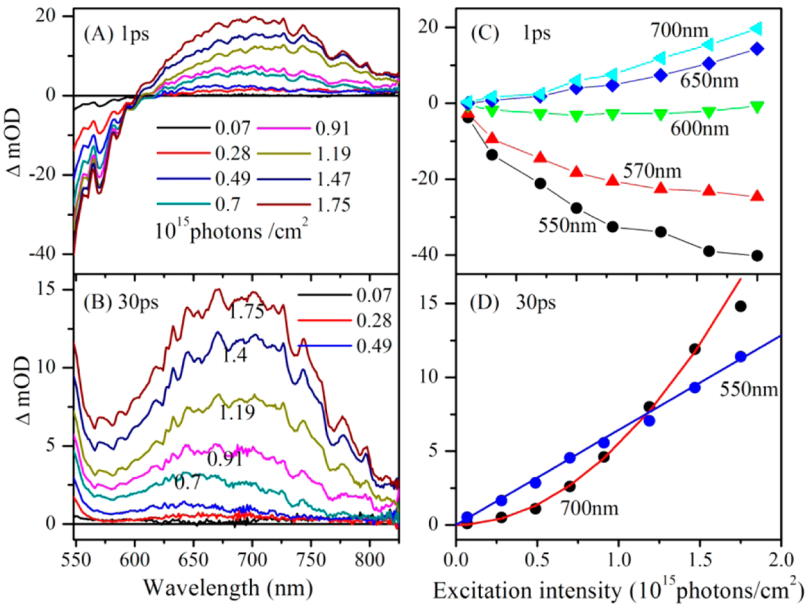

Figure 3. Excitation−intensity dependence of the solvated-electron absorption. (A) Transient spectra in the visible-near-infrared region at a pump−probe delay of 1 ps as a function of excitation intensity. (B) Transient spectra at a pump−probe delay 30 ps as a function of excitation intensity. (C) Change in absorption as a function of excitation intensity at selected wavelengths, at a pump−probe delay of 1 ps. (D) Change in absorption as a function of excitation intensity at 550 and 700 nm at a pump−probe delay of 30 ps. Dots are experimental data, the red line is the fitted curve with $y = 5.51x^2$, and the blue line is the fitted curve with $y = 6.43x$.

the experiment on the water buffer only. This signal, the magenta curve in Figure 2A, revealed no solvated electrons, even when the excitation intensity was increased three-fold. Note that the signal from the counterpart of the liberated electron, the pCa neutral species, which has been reported to absorb near 370 nm[12,13,21−23] similar to the absorption of the phenolate anion after photoionization,[19] is outside the current spectral window.

Figure 3A presents the excitation intensity dependence of the signal at an early time delay of 1 ps. Clearly, the pump−probe signal displays nonlinear behavior, as demonstrated more clearly in Figure 3C. At a later delay time of 30 ps, when the excited-state emission had decayed completely, a quadratic intensity dependence was observed at wavelengths longer than 580 nm, where the absorption can be attributed purely to solvated electrons; see Figure 3B,D. Thus, the ionization was confirmed to occur via a two-photon absorption process at 400 nm. At wavelengths shorter than 550 nm, a linear relationship was observed (Figure 3D), indicating that at long delay time the solvated electron absorption does not contribute much to the visible region. This explains why the expected[12,13,23] excitation energy dependence was not observed in previous experiments. The mixed nonlinear behavior of the saturation curves at short time delay, in Figure 3C, shows that signals that form the excited states contribute to the nearIR region, and a clean dissection can be made only at longer delay times.

The ground-state absorption of PYP peaks around 445 nm (2.8 eV), as shown in Figure 1, whereas in Figure 2A, an excited-state absorption peaks around ∼380 nm (3.3 eV), and thus a higher excited state 6.1 eV above the ground state must exist. The generation of the hydrated electrons most likely occurs resonantly via the excited state at 380 nm in a sequential two-photon absorption process.[12] However, previously, a pseudolinear power dependence was observed.[12] Here we observe the quadratic intensity dependence, illustrated in Figure 3D, expected for a two-photon excitation mechanism as we have a clean probe of the electron signal around 700 nm after 30 ps. Population of the higher excited state by absorption of two photons of 400 nm (∼6.2 eV) apparently leads to electron ejection from the chromophore. To decide whether this higher excited state has a charge-transfer-to-solvent character that leads to ejection of the electron after a delay or is an ionizing state that ejects electrons immediately needs further investigation. Our current time resolution (∼200 fs) is unable to resolve this process. Supra-molecular ab initio calculations of different pCa analogues show that the IP is a significant property of the pCa electronic structure.[14] Therefore, we temporally ascribe the electron-ejection process to a direct photoionization induced by two-photon absorption at 400 nm. Interestingly though, the predicted strong dependence of the IP level on protein environment[14] is not confirmed, as similar two-photon ionization has been observed in pump−probe studies of a solution containing isolated PYP chromophore analogs using 395 nm excitation.[22,23]

To resolve the electron dynamics from the one-photon reaction channel in the visible-near-infrared region, we globally fitted data with high excitation intensity with two sequentially decaying branches in parallel, as shown in Figure 4A. The first branch represented the two-photon electron channel, and the second represented the one-photon excited-state channel. Figure 4B exhibits several time decay traces at selected wavelengths with globally fitted results. As shown in Figure 4A, the separation between the one-photon and two-photon channel worked quite well. The black and red curves of the stimulated emission tail of the one-photon excited state had a lifetime of 480 fs and 1.7 ps respectively, consistent with previous observations[12,31] and our observation at low excitation intensity (Figure S1 in the Supporting Information) in the excited-state emission region. In the two-photon electron branch, the first spectrum had a lifetime ∼12 ps and decayed into the second spectrum, which had a lifetime (∼4 ns) longer

dx.doi.org/10.1021/jp311906f | J. Phys. Chem. B XXXX, XXX, XXX−XXX

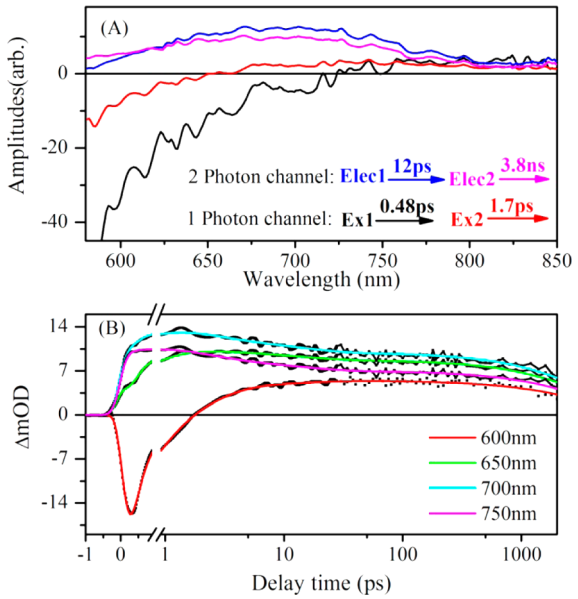

Figure 4. (A) Species spectra of one- and two-photon channel extracted by global fitting of the data at high excitation intensity, $I \approx 1.5 \times 10^{15}$ photons/cm^2, to the model displayed in the inset. The spectra are color-coded with the model. (B) Representative time traces and fit to the data using the model in panel A.

than our detection time window. Both spectra have a band shape similar to the observed raw data at long delay times.

The global target fitting based on first-order kinetics provides a satisfactory phenomenological description. To characterize further the electron-radical recombination dynamics, similarly as in solvents, a classic model based on Fick's second law of diffusion[35] can be used to reproduce the geminate recombination dynamics. In general, geminate recombination of independent pairs is given by the solution to the diffusion equation developed by Collins and Kimball[36,37]

$$\frac{\partial C(r,t)}{\partial t} = D\nabla^2 C(r,t) \tag{1}$$

where D is the sum of the diffusion coefficients of the electron and the chromophore radical and $C(r,t)$ represents the time- and space-resolved survival probability function. With a boundary condition $C(R,t) = 0$, that is, at a given reaction radius R where the recombination is assumed to be instantaneous, the solution of 1 is given by

$$C(r,t) = C_0\left[1 - \frac{R}{r}\,\mathrm{erfc}\left(\frac{r-R}{\sqrt{4Dt}}\right)\right] \tag{2}$$

here erfc is the complementary error function. By assuming the initial distribution of the electrons to be an exponential form

$$C_0 = \frac{\exp(-r/b)}{8\pi b^3} \tag{3}$$

where the average radius of the distribution is $3b$. Thus, the final time-resolved survival probability of the ionized electron can be expressed as

$$C(t) = \int_R^\infty \frac{\exp(-r/b)}{8\pi b^3} \times \left[1 - \frac{R}{r}\,\mathrm{erfc}\left(\frac{r-R}{\sqrt{4Dt}}\right)\right] \times 4\pi r^2\,\mathrm{d}r \tag{4}$$

Here $C(t)$ in eq 4 represents the time-resolved survival probability of the solvated electron that has not recombined with the radical, which is corresponding to our experimental observation of the solvated electrons. With formula 4 and a fixed recombination distance of R = 2 Å (radius of the oxygen anion), the decay dynamics at 700 nm in the first 500 ps range and the fraction of geminately recombining electrons were well-reproduced, with the parameters shown in Figure 5A and the initial ejected electron distribution depicted in Figure 5B.

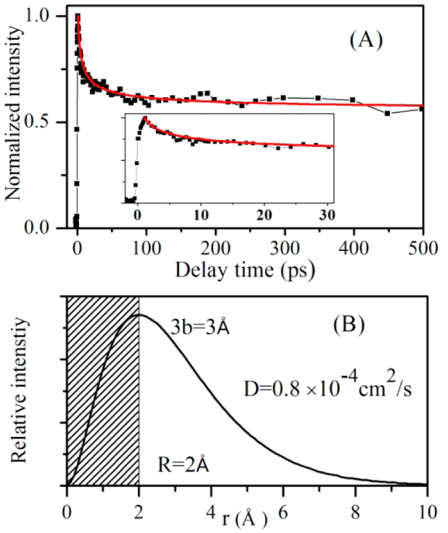

Figure 5. Simulated electron and radical recombination dynamics in (A) (red line, at 700 nm) and initial electron distribution in (B). Recombination distance was fixed at R = 2.

According to the simulated results, the electron is ejected to an average distance of ~3 Å ($3b$) away from the radical center. Because the recombination is a nonadiabatic process,[37] the electron must return to the ground state of the anion. The small values of R and $3b$ would indicate that the electron is located quite close to its recombination center. The other fraction of the electrons, which survives out on to long delay time, does not primarily geminately recombine. These electrons could transiently combine with a low-redox potential residue, be stabilized by nearby amino-acid residues, or escape out of the protein pocket, and they finally recombine with other centers.

Inside PYP, diffusion of the chromophore radical can be ignored in comparison with the electron, and thus D is determined by the electron only and depends on the environment inside the protein. The simulated D is ~0.8 × 10^{-4} cm^2/s, or 0.8 Å^2/ps, in the order of the diffusion coefficient of the solvated electron in pure water, which has a measured value of ~0.5 Å^2/ps.[38,39] This indicates that either the amino acids solvating the electron provide an environment similar to that of water or, although buried inside the protein pocket, the chromophore is surrounded by water molecules. In the crystal structure of PYP, at least one water molecule (water 200) is observed, which is nevertheless far from the active site.[40] In water solvent, the conformation of the protein may be more loose and flexible than in the crystal packing, which may cause water molecules to penetrate in the active site. While so far no other experimental study has referred to water molecules in the cavity of PYP under water solvent conditions, theoretical simulations on mutants provide support for this hypothesis.

dx.doi.org/10.1021/jp311906f | J. Phys. Chem. B XXXX, XXX, XXX–XXX

Molecular dynamics simulations on wild type and mutants of PYP indicated that around three water molecules are present in the active site within a 3.5 Å range of the chromophore, which enter via the amino residues P68 or E46.[30] Therefore, it is possible that water molecules in the PYP cavity in combination with hydrogen bonds from protein residues provide an environment similar to water solvent, in which fast individual reorientational solvent motions under the influence of thermal fluctuations determine the electron diffusion rate.[41]

To test whether the protein residues around the chromophore modulate the local environment of the electron, the electron recombination kinetics were measured in two mutants, E46Q and P68F. (See Figures S2 and S3 in the Supporting Information.) In mutant E46Q, the glutamic acid residue 46 is replaced by glutamine, resulting in a slightly weaker hydrogen bond with the phenol ring of pCa and a red shift of the pCa absorption of ∼15 nm, as shown in Figure S3 in the Supporting Information. In mutant P68F, residue proline 68 is replaced by phenylanine. This mutation is expected to keep the interaction between pCa and the protein untouched at the phenol side of pCa, whereas it may change the conditions around the carbonyl side of pCa. This mutant is similar to mutants P68V, P68A, and P68G[30] used in a previous study that showed that residue p68 in PYP has an important role in restricting the access of water molecules to the chromophore-binding pocket and pCa and thus exerts a positive influence on the photoisomerization yield in PYP. However, side chain of phenylanine is larger in size and is more hydrophobic than the one of alanine, glycine, and valine.

As shown in Figure 6A, in both of the mutants the absorption spectrum of the solvated electron is similar to that of wild-type PYP, with only a slight red shift or narrowing. In mutant E46Q, the electron-radical recombination was more or less the same as that in wild-type PYP, whereas in the mutant P68F, the fraction of electrons that recombine on a faster time scale became significantly larger than in wild-type PYP, as depicted in Figure 6B. If the initial electron distribution would be the same in all three types of protein, then the observed more extensive geminate recombination in P68F would indicate that the diffusion rate of the electron is slower than that in WT and in E46Q. Because the steady-state absorption (Figure S3 in the Supporting Information) demonstrates only a slight shift and the hydrogen bond at the chromophore phenolate side has not been changed, the IP of pCa in PYP-P68F would not be expected to change much, and thus indeed the injection of an electron may be expected to form an initial distribution similar to WT. Thus, for the sake of simplicity, a diffusion simulation was performed for P68F using the same initial electron distribution as in wild-type PYP, resulting in a good-quality simulation of the data, as shown by the blue line in Figure 6B. The simulation yielded as expected a diffusion constant slower than that in WT and E46Q, of $D \approx 0.15$ Å^2/ps. This slower electron diffusion in P68F may be caused by the interaction of the electron with more water molecules that solvate, or trap, the electron more effectively near the chromophore. This will decrease its chance to escape out of the protein cavity and thus increase the chance to recombine with the radical inside the protein cavity. If we compare with the MD simulations of the other P68 mutants,[30] then we may speculate that the larger number of water molecules near the protein backbone and residue 68 block the exit for the electron. However, a more detailed modeling of this mutant and the fate of a solvated electron in PYP are needed to understand the dynamics of the solvated electron better and to advance the understanding and modeling of protein-chromophore dynamics.

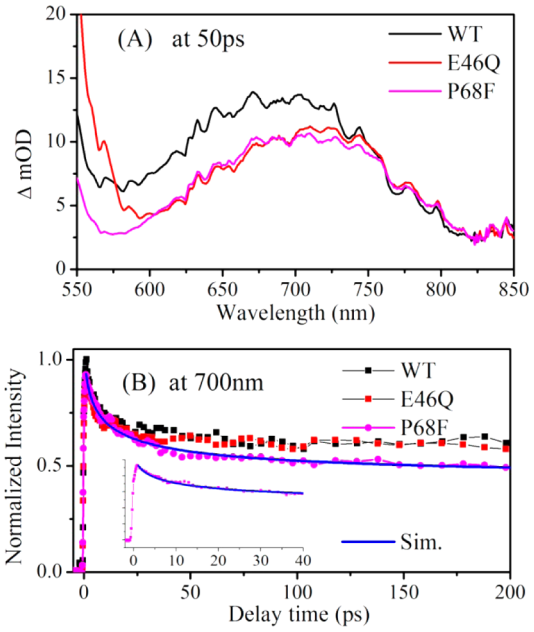

Figure 6. (A) Solvated electron absorption band in wild-type PYP and mutants E46Q and P68F. (B) Dynamics of solvated electrons and simulation result for P68F. The simulation parameters were similar to wild-type PYP but with $D = 0.15$ Å^2/ps.

In summary, we have studied photoionization and geminate electron-radical recombination dynamics in PYP. An absorption band extending from 550 to 850 nm was observed and assigned to absorption from solvated electrons, ejected upon two-photon excitation of the pCa chromophore. The solvated electron showed decay dynamics that could be simulated with a diffusion equation for geminate recombination. From the simulation, we conclude that the electron is ejected to a location ∼3 Å from the ejection center and recombination occurs at a short distance of ∼2 Å and is controlled by diffusion. The simulated diffusion coefficient is an indication that the diffusion behavior of the solvated electrons inside PYP is similar to that in aqueous solvent environment, slightly modified by the dielectric environment of the protein residues. Results on mutant PYPs corroborate that proline 68 has an important role in controlling water molecules entering the protein pocket around the chromophore.

■ ASSOCIATED CONTENT

Supporting Information

Experimental methods, data analysis, mutant structures, and absorption spectra. This material is available free of charge via the Internet at http://pubs.acs.org.

■ AUTHOR INFORMATION

Corresponding Author

*E-mail: m.l.groot@vu.nl.

Notes

The authors declare no competing financial interest.

dx.doi.org/10.1021/jp311906f | J. Phys. Chem. B XXXX, XXX, XXX−XXX

■ ACKNOWLEDGMENTS

This research was supported by The Netherlands Organization for Scientific Research via the Dutch Foundation for Earth and Life Sciences (Investment Grant no. 834.01.002 and grant no. 819.02.001). We thank Mr. J. Thieme for assistance in the lab

■ REFERENCES

(1) Meyer, T. E.; Tollin, G.; Hazzard, J. H.; Cusanovich, M. A. Photoactive Yellow Protein from the Purple Phototrophic Bacterium, *Ectothiorhodospira halophila*. Quantum Yield of Photobleaching and Effects of Temperature, Alcohols, Glycerol, And Sucrose on Kinetics of Photobleaching and Recovery. *Biophys. J.* **1989**, *56*, 559−564.

(2) Cusanovich, M. A.; Meyer, T. E. Photoactive Yellow Protein: A Prototypic PAS Domain Sensory Protein and Development of a Common Signaling Mechanism. *Biochemistry* **2003**, *42*, 4759−4770.

(3) Sprenger, W. W.; Hoff, W. D.; Armitage, J. P.; Hellingwerf, K. J. The Eubacterium *Ectothiorhodospira halophila* Is Negatively Phototactic, With a Wavelength Dependence That Fits the Absorption Spectrum of the Photoactive Yellow Protein. *J. Bacteriol.* **1993**, *175*, 3096−3104.

(4) Hellingwerf, K. J.; Hendriks, J.; Gensch, T. Photoactive Yellow Protein, A New Type of Photoreceptor Protein: Will This "Yellow Lab" Bring Us Where We Want to Go? *J. Phys. Chem. A* **2003**, *107*, 1082−1094.

(5) Stahl, A. D.; Hospes, M.; Singhal, K.; van Stokkum, I.; van Grondelle, R.; Groot, M. L.; Hellingwerf, K. J. On the Involvement Of Single-Bond Rotation in the Primary Photochemistry of Photoactive Yellow Protein. *Biophys. J.* **2011**, *101*, 1184−1192.

(6) Larsen, D. S.; van Grondelle, R. Initial Photoinduced Dynamics of the Photoactive Yellow Protein. *ChemPhysChem* **2005**, *6*, 828−837.

(7) Genick, U. K.; Soltis, S. M.; Kuhn, P.; Canestrelli, I. L.; Getzoff, E. D. Structure At 0.85 A Resolution of an Early Protein Photocycle Intermediate. *Nature* **1998**, *392*, 206−209.

(8) Van Brederode, M. E.; Hoff, W. D.; Van Stokkum, I. H.; Groot, M. L.; Hellingwerf, K. J. Protein Folding Thermodynamics Applied to the Photocycle of the Photoactive Yellow Protein. *Biophys. J.* **1996**, *71*, 365−380.

(9) Groot, M. L.; van Wilderen, L.; Larsen, D. S.; van der Horst, M. A.; van Stokkum, I. H. M.; Hellingwerf, K. J.; van Grondelle, R. Initial Steps of Signal Generation in Photoactive Yellow Protein Revealed with Femtosecond Mid-Infrared Spectroscopy. *Biochemistry* **2003**, *42*, 10054−10059.

(10) van Wilderen, L.; Van der Horst, M. A.; van Stokkum, I. H. M.; Hellingwerf, K. J.; van Grondelle, R.; Groot, M. L. Ultrafast Infrared Spectroscopy Reveals a Key Step for Successful Entry into the Photocycle for Photoactive Yellow Protein. *Proc. Natl. Acad. Sci. U. S. A.* **2006**, *103*, 15050−15055.

(11) Verhoefen, M. K.; Neumann, K.; Weber, I.; Glaubitz, C.; Wachtveitl, J. Primary Reaction Dynamics of Proteorhodopsin Mutant D97N Observed by Femtosecond Infrared and Visible Spectroscopy. *Photochem. Photobiol.* **2009**, *85*, 540−546.

(12) Larsen, D. S.; van Stokkum, I. H. M.; Vengris, M.; van der Horst, M. A.; de Weerd, F. L.; Hellingwerf, K. J.; van Grondelle, R. Incoherent Manipulation of the Photoactive Yellow Protein Photocycle with Dispersed Pump-Dump-Probe Spectroscopy. *Biophys. J.* **2004**, *87*, 1858−1872.

(13) Lincoln, C. N.; Fitzpatrick, A. E.; Thor, J. J. Photoisomerisation Quantum Yield and Non-Linear Cross-Sections with Femtosecond Excitation of the Photoactive Yellow Protein. *Phys. Chem. Chem. Phys.* **2012**, *14*, 15752−15764.

(14) Gromov, E. V.; Burghardt, I.; Koppel, H.; Cederbaum, L. S. Electronic Structure of the PYP Chromophore in Its Native Protein Environment. *J. Am. Chem. Soc.* **2007**, *129*, 6798−6806.

(15) Gromov, E. V.; Burghardt, I.; Hynes, J. T.; Koppel, H.; Cederbaum, L. S. Electronic Structure of the Photoactive Yellow Protein Chromophore: Ab Initio Study of the Low-Lying Excited Singlet States. *J. Photoch. Photobiol., A* **2007**, *190*, 241−257.

(16) Baltuska, A.; Emde, M. F.; Pshenichnikov, M. S.; Wiersma, D. A. Early-Time Dynamics of the Photoexcited Hydrated Electron. *J. Phys. Chem. A* **1999**, *103*, 10065−10082.

(17) Long, F. H.; Shi, X. L.; Lu, H.; Eisenthal, K. B. Electron Photodetachment from Halide-Ions in Solution - Excited-State Dynamics in the Polarization Well. *J. Phys. Chem.* **1994**, *98*, 7252−7255.

(18) Sauer, M. C.; Crowell, R. A.; Shkrob, I. A. Electron Photodetachment from Aqueous Anions. 1. Quantum Yields for Generation of Hydrated Electron by 193 and 248 nm Laser Photoexcitation of Miscellaneous Inorganic Anions. *J. Phys. Chem. A* **2004**, *108*, 5490−5502.

(19) Chen, X. Y.; Larsen, D. S.; Bradforth, S. E.; van Stokkum, I. H. M. Broadband Spectral Probing Revealing Ultrafast Photochemical Branching after Ultraviolet Excitation of the Aqueous Phenolate Anion. *J. Phys. Chem. A* **2011**, *115*, 3807−3819.

(20) Iglev, H.; Fischer, M. K.; Gliserin, A.; Laubereau, A. Ultrafast Geminate Recombination after Photodetachment of Aqueous Hydroxide. *J. Am. Chem. Soc.* **2011**, *133*, 790−795.

(21) Larsen, D. S.; Vengris, M.; van stokkum, I. H. M.; van der Horst, M.; Cordfunke, R.; Hellingwerf, K. J.; van Grondelle, R. Initial Photo-Induced Dynamics of the Photoactive Yellow Protein Chromophore in Solution. *Chem. Phys. Lett.* **2003**, *369*, 563−569.

(22) Changenet-Barret, P.; Plaza, P.; Martin, M. M. Primary Events In The Photoactive Yellow Protein Chromophore In Solution. *Chem. Phys. Lett.* **2001**, *336*, 439−444.

(23) Larsen, D. S.; Vengris, M.; van Stokkum, I. H. M.; van der Horst, M. A.; de Weerd, F. L.; Hellingwerf, K. J.; van Grondelle, R. Photoisomerization and Photoionization of the Photoactive Yellow Protein Chromophore in Solution. *Biophys. J.* **2004**, *86*, 2538−2550.

(24) Schutz, C. N.; Warshel, A. What Axe the Dielectric "Constants" of Proteins and How to Validate Electrostatic Models? *Proteins* **2001**, *44*, 400−417.

(25) Hellingwerf, K. J.; van Thor, J. J.; Hoff, W. D.; Hendriks, J. In *Nanotechnology: Towards a Molecular Construction Kit*; Netherlands Study Centre for Technology Trends (STT): The Hague, The Netherlands, 1998.

(26) Kort, R.; Hoff, W. D.; Van West, M.; Kroon, A. R.; Hoffer, S. M.; Vlieg, K. H.; Crielaand, W.; Van Beeumen, J. J.; Hellingwerf, K. J. The Xanthopsins: A New Family of Eubacterial Blue-Light Photoreceptors. *Embo. J.* **1996**, *15*, 3209−3218.

(27) van Aalten, D. M.; Haker, A.; Hendriks, J.; Hellingwerf, K. J.; Joshua-Tor, L.; Crielaard, W. Engineering Photocycle Dynamics. Crystal Structures and Kinetics of Three Photoactive Yellow Protein Hinge-Bending Mutants. *J. Biol. Chem.* **2002**, *277*, 6463−6468.

(28) Bonetti, C.; Stierl, M.; Mathes, T.; van Stokkum, I. H.; Mullen, K. M.; Cohen-Stuart, T. A.; van Grondelle, R.; Hegemann, P.; Kennis, J. T. The Role of Key Amino Acids in the Photoactivation Pathway of the Synechocystis Slr1694 BLUF Domain. *Biochemistry* **2009**, *48*, 11458−11469.

(29) van Stokkum, I. H.; Larsen, D. S.; van Grondelle, R. Global and Target Analysis of Time-Resolved Spectra. *Biochim. Biophys. Acta* **2004**, *1657*, 82−104.

(30) Rupenyan, A. B.; Vreede, J.; van Stokkum, I. H.; Hospes, M.; Kennis, J. T.; Hellingwerf, K. J.; Groot, M. L. Proline 68 Enhances Photoisomerization Yield in Photoactive Yellow Protein. *J. Phys. Chem. B* **2011**, *115*, 6668−6677.

(31) Changenet-Barret, P.; Plaza, P.; Martin, M. M.; Chosrowjan, H.; Taniguchi, S.; Mataga, N.; Imamoto, Y.; Kataoka, M. Structural Effects on the Ultrafast Photoisomerization of Photoactive Yellow Protein. Transient Absorption Spectroscopy of Two Point Mutants. *J. Phys. Chem. C* **2009**, *113*, 11605−11613.

(32) Jou, F. Y.; Freeman, G. R. Temperature and Isotope Effects on the Shape of the Optical-Absorption Spectrum of Solvated Electrons in Water. *J. Phys. Chem.* **1979**, *83*, 2383−2387.

(33) Pepin, C.; Goulet, T.; Houde, D.; JayGerin, J. P. Observation of a Continuous Spectral Shift in the Solvation Kinetics of Electrons in Neat Liquid Deuterated Water. *J. Phys. Chem. A* **1997**, *101*, 4351−4360.

(34) Hart, E. J.; Boag, J. W. Absorption Spectrum of Hydrated Electron in Water and in Aqueous Solutions. *J. Am. Chem. Soc.* **1962**, *84*, 4090−4095.
(35) Fick, A. On Liquid Diffusion (Reprinted from the London, Edinburgh, and Dublin Philosophical Magazine and Journal of Science, Vol 10, Pg 30, 1855). *J. Membr. Sci.* **1995**, *100*, 33−38.
(36) Collins, F. C.; Kimball, G. E. Diffusion-Controlled Reaction Rates. *J. Coll. Sci., Imp. Univ. Tokyo* **1949**, *4*, 425−437.
(37) Kloepfer, J. A.; Vilchiz, V. H.; Lenchenkov, V. A.; Germaine, A. C.; Bradforth, S. E. The Ejection Distribution of Solvated Electrons Generated by the One-Photon Photodetachment of Aqueous I- and Two-Photon Ionization of the solvent. *J. Chem. Phys.* **2000**, *113*, 6288−6307.
(38) Schmidt, K. H.; Han, P.; Bartels, D. M. Temperature-Dependence of Solvated Electron-Diffusion in H_2O and D_2O. *J. Phys. Chem.* **1992**, *96*, 199−206.
(39) Schmidt, K. H.; Han, P.; Bartels, D. M. Radiolytic Yields of the Hydrated Electron from Transient Conductivity - Improved Calculation of the Hydrated Electron-Diffusion Coefficient and Analysis of Some Diffusion-Limited $(e^-)_{aq}$ Reaction-Rates. *J. Phys. Chem.* **1995**, *99*, 10530−10539.
(40) Kandori, H.; Iwata, T.; Hendriks, J.; Maeda, A.; Hellingwerf, K. J. Water Structural Changes Involved in the Activation Process of Photoactive Yellow Protein. *Biochemistry* **2000**, *39*, 7902−7909.
(41) Tay, K. A.; Coudert, F. X.; Boutin, A. Mechanism and Kinetics of Hydrated Electron Diffusion. *J. Chem. Phys.* **2008**, *129*, 054505(1)−054505(7).